Neuro-Oncology

21(2), 274–284, 2019 | doi:10.1093/neuonc/noy098 | Advance Access date 9 June 2018

274

Dynamic ^{18}F-FET PET is a powerful imaging biomarker in gadolinium-negative gliomas

Mathias Kunz, Nathalie Lisa Albert, Marcus Unterrainer, Christian la Fougere, Rupert Egensperger, Ulrich Schüller, Juergen Lutz, Simone Kreth, Jörg-Christian Tonn, Friedrich-Wilhelm Kreth, and Niklas Thon

Department of Neurosurgery (M.K., J.C.T., F.W.K., N.T.), Department of Nuclear Medicine (N.L.A., M.U., C.L.F.), Center for Neuropathology (R.E., U.S.), Department of Clinical Radiology (J.L.), Department of Anaesthesiology (S.K.), University of Munich, Munich, Germany; German Cancer Consortium, partner site Munich, Germany (M.K., N.L.A., M.U., R.E., J.C.T., F.W.K., N.T.); Division of Nuclear Medicine and Clinical Molecular Imaging, Department of Radiology, University of Tübingen, Tübingen, Germany (C.L.F.); Department of Pediatric Hematology and Oncology, University Medical Center Hamburg-Eppendorf, Hamburg, Germany (U.S.); Institute of Neuropathology, University Medical Center Hamburg-Eppendorf, Hamburg, Germany (U.S.); Research Institute Children's Cancer Center Hamburg, Hamburg, Germany (U.S.)

Corresponding Author: Friedrich-Wilhelm Kreth, MD, Department of Neurosurgery, University of Munich—Campus Grosshadern, Germany (Friedrich-Wilhelm.Kreth@med.uni-muenchen.de).

Abstract

Background. We aimed to elucidate the place of dynamic O-(2-[^{18}F]-fluoroethyl)-L-tyrosine (^{18}F-FET) PET in prognostic models of gadolinium (Gd)-negative gliomas.

Methods. In 98 patients with Gd-negative gliomas undergoing ^{18}F-FET PET guided biopsy, time activity curves (TACs) of each tumor were qualitatively categorized as either increasing or decreasing. Additionally, post-hoc quantitative analyses were done using minimal time-to-peak (TTP_{min}) measurements. Prognostic factors were obtained from multivariate hazards models. The fit of the biospecimen- and imaging-derived models was compared.

Results. A homogeneous increasing, mixed, and homogeneous decreasing TAC pattern was seen in 51, 19, and 28 tumors, respectively. Mixed TAC tumors exhibited both increasing and decreasing TACs. Corresponding adjusted 5-year survival was 85%, 47%, and 19%, respectively ($P < 0.001$). Qualitative and quantitative TAC measurements were highly intercorrelated ($P < 0.0001$). TTP_{min} was longest (shortest) in the homogeneous increasing (decreasing) TAC group and in between in the mixed TAC group. TTP_{min} was longer in isocitrate dehydrogenase (*IDH*)-mutant tumors ($P < 0.001$). Outcome was similarly precisely predicted by biospecimen- and imaging-derived models. In the biospecimen model, World Health Organization (WHO) grade ($P < 0.0001$) and *IDH* status ($P < 0.001$) were predictors for survival. Outcome of homogeneous increasing (homogeneous decreasing) TAC tumors was nearly identical, with both $TTP_{min} > 25$ min ($TTP_{min} \leq 12.5$ min) tumors and *IDH*-mutant grade II (*IDH*-wildtype) gliomas. Outcome of mixed TAC tumors matched that of both intermediate TTP_{min} (>12.5 min and ≤25 min) and *IDH*-mutant, grade III gliomas. Each of the 3 prognostic clusters differed significantly from the other ones of the respective models ($P < 0.001$).

Conclusion. TAC measurements constitute a powerful biomarker independent from tumor grade and *IDH* status.

Keywords

^{18}F-FET PET | biomarkers | glioma | prognosis | targeted therapy

Gadolinium (Gd)-negative gliomas remain a diagnostic and therapeutic challenge.[1–4] Clinical outcome is highly divergent and predominantly determined by molecular and histopathological profiles.[1,5–9] Conventional MRI, which represents the mainstay for diagnosis and management of gliomas, lacks prognostic power in Gd-negative gliomas.[1,10–12] Thus, there is an urgent need for additional imaging biomarkers.[13,14]

Importance of the study

The prognosis of Gd-negative gliomas varies widely and is determined by histopathology and molecular-genetic profiles. The current study indicates that advanced imaging techniques such as dynamic ^{18}F-FET-PET can provide prognostic information independent of WHO grade and *IDH* mutational status. Adjusted and unadjusted survival estimates relying either on WHO grade and *IDH* mutational status or alternatively on TACs of dynamic ^{18}F-FET-PET resulted in a 3-scaled outcome pattern, which was well matched across the models. Our data provide evidence of dynamic ^{18}F-FET-PET as a prognostic imaging biomarker. Our findings open new avenues for patient counseling and treatment planning.

In the past decade, positron emission tomography (PET) has been established as an important diagnostic tool in the management of gliomas.[15] In our initial published study, we demonstrated that the intratumoral uptake of the radiolabeled amino acid O-(2-[^{18}F]-fluoroethyl)-L-tyrosine (^{18}F-FET) over time (aka "time activity curves" [TACs]) can be characterized by 3 distinct patterns in Gd-negative tumors: (i) a homogeneously increasing, (ii) a homogeneously decreasing, and (iii) a mixed pattern with both increasing and decreasing TACs within the same tumor.[16] In our recently published follow-up evaluation, we found associations between TAC patterns and progression-free survival (PFS): homogeneous increasing TAC tumors experienced favorable PFS and those with decreasing TAC significantly worse PFS.[17] However, no significant PFS difference was seen between mixed and homogeneous decreasing TAC tumors and no valid death rate estimation was possible due to the short follow-up period. Thus, the place of the reported 3-scaled TAC pattern in prognostic models of Gd-negative gliomas still needs elucidation. For clarification the current long-term analysis was conducted. We here analyzed the prognostic impact of TAC within the framework of the molecular markers implemented in the 2016 revision of the World Health Organization (WHO) classification scheme for brain tumors.[5] As recently published studies have pointed to the prognostic importance of quantitative TAC analyses,[18,19] we did additionally post-hoc quantitative analyses of TAC in terms of minimal time-to-peak (TTP_{min}) measurements to elucidate and compare the strengths, similarities, and differences of qualitative and quantitative TAC data in prognostic models of Gd-negative gliomas. We further assessed the usefulness of TAC-defined targets for surgical guidance and did post-hoc analyses on the efficacy of treatment strategies among patients exhibiting the same/distinct TAC patterns.

Methods

Patients

The design of this prospective single center study has been described in detail before.[16,17] In brief, patients with MRI-suspected Gd-negative low-grade glioma exhibiting increased ^{18}F-FET uptake (compared with the corresponding area in the non-affected contralateral hemisphere) were included. MRI-suspected low-grade gliomas were defined as hyperintense (hypointense) Gd-negative lesions in T_2 (T_1)-weighted sequences exhibiting space occupying effects. Patients were enrolled between February 2006 and September 2010. Informed consent was obtained from all patients. The study protocol was reviewed and approved by the ethical review board of the Ludwig-Maximilians University in Munich, Germany (AZ 216/14).

^{18}F-FET-PET Protocol

A detailed description has been presented before.[17] In brief, an ECAT EXACT HR+ scanner (Siemens Healthineers) was used in all patients. Following a 15 min transmission scan (germanium-68 rotating rod source), a 40 min long dynamic emission recording in 3D mode was started immediately after intravenous bolus injection of approximately 180 MBq ^{18}F-FET. PET data were reconstructed by filtered back projection and corrected for attenuation, scatter, random, and dead time. Dynamic PET data were acquired using predefined time frames (7 × 10 s, 3 × 30 s, 1 × 2 min, 3 × 5 min, 2 × 10 min). Spatial resolution of ^{18}F-FET PET was 2.0 mm × 2.0 mm × 1.0 mm per pixel with a center-center separation of 1.2 pixel. PET data were routinely coregistered with MRI and evaluated at the work station (Hermes Medical Solutions). Investigators were blinded for clinical, histological, and molecular data. Maximal ^{18}F-FET uptakes within the tumor (expressed as maximal standardized uptake value [SUV_{max}]) were determined on late summation images (20–40 min post-tracer injection [p.i.]), and maximal tumor to mean background (BG) ratios (SUV_{max}/BG) were calculated. For dynamic analyses the early summation image (10–30 min p.i.) were used for the definition of a 90% isocontour threshold region of interest (ROI). Subsequently, these ROIs were applied to the corresponding slices of the entire dynamic PET images to extract individual TACs for the kinetic analysis in a slice-by-slice manner. Each TAC within the slice-by-slice analyses during the 40 min time interval after tracer injection was defined as follows: (i) increasing TAC with SUV constantly ascending or reaching a peak followed by a plateau in the subsequent frames (±3% of the peak SUV) and (ii) decreasing TAC with SUV showing an early peak followed by a constant descent thereafter. Early fluctuations in the TACs within the first short time frames (7 × 10 s followed by 3 × 30 s) representing noise were excluded from kinetic analyses. Each tumor was mapped per its intratumoral TAC patterns: Tumors with increasing TAC in all slices throughout the

whole tumor were classified as having homogeneously increasing kinetics, tumors with decreasing TAC in all slices throughout the whole tumor were considered as having homogeneously decreasing kinetics, and tumors with both increasing and decreasing TAC slices were classified as having a mixed TAC pattern. The prospectively performed qualitative categorization of TAC was supplemented by blinded, post-hoc quantitative TAC analyses in terms of TTP_{min} measurements. Both the initial qualitative and the post-hoc quantitative TAC analyses were done by 2 experienced nuclear physicians. In case of different findings, a conference was initiated in order to reach consensus. For each patient included in this study, TTP was assessed in each slice throughout the whole tumor; consequently, the shortest TTP in at least 2 consecutive slices was defined as TTP_{min} as previously published.[20]

To estimate the approximate volume of focal decreasing TAC (hot spot) in heterogeneously composed tumors, areas showing decreasing TAC were segmented in each individual slice on the static PET images by means of a semiautomatic threshold-based calculation (SUV/BG ≥ 1.8). For further biopsy planning, the center of the hot spot was labeled in the corresponding PET data by means of a 9 × 9 mm square marker.

PET-Guided Stereotactic Biopsy Protocol

At the time of the initial presentation, all patients underwent ^{18}F-FET-PET–guided serial stereotactic biopsy procedures, as described previously.[16,21] Trajectory planning was based on coregistered multimodal imaging data including computed tomography (CT), MRI, and 3D dynamic ^{18}F-FET uptake data (i-plan stereotaxy, Brainlab). The applied MRI protocol has been described previously.[16] Serial biopsy samples (1 mm^3 in size) were collected in 1 mm steps along the trajectory for representative tissue sampling. Tumor samples were collected from areas exhibiting the same/different ^{18}F-FET uptake kinetics (eg, "hot spots" with decreasing TAC embedded within tumor areas with increasing TAC). Histopathological examination was done in a blinded fashion unaware of the PET findings. Samples selected for histological examination were paraffin embedded, whereas for molecular-genetic analyses at least 2 snap-frozen samples were used. Each of the collected samples was tagged according to its exact location within the stereotactically localized 3D imaging matrix, allowing correlative analyses between areas of similar/different histopathological and molecular-genetic findings and their corresponding TAC patterns.

Histology and Molecular Markers

All patients were grouped according to histopathology and molecular profiles as being recommended by the 2016 WHO classification of brain tumors.[5] *IDH*-mutational status was determined by pyrosequencing, 1p/19q codeletion status by microsatellite analysis, and O^6-methylguanine-DNA methyltransferase (*MGMT*) promoter methylation status by methylation-specific PCR and bisulfite sequencing. In addition, the telomerase reverse transcriptase (*TERT*) mutational status was determined in *IDH*-wildtype tumors by PCR and sequencing.[21]

Patient Management

All treatment decisions were made by the interdisciplinary tumor board under consideration of patient- and tumor-related covariates (eg, Karnofsky performance status [KPS], tumor location, histological diagnosis, the molecular biomarker profile). PET data were not part of the standardized treatment algorithm. Circumscribed tumors were generally considered for open tumor resection or alternatively (in case of small sized and complex located gliomas) for stereotactic brachytherapy.[22] WHO grade II gliomas with diffuse extensions and/or functionally eloquent locations exhibiting favorable molecular profiles (ie, 1p/19q codeletion) and all IDH-mutant WHO grade III gliomas usually underwent upfront chemotherapy rather than radiation therapy.[23] *IDH*-wildtype anaplastic gliomas and all WHO grade IV glioblastomas were commonly treated with radiotherapy plus concomitant and adjuvant temozolomide.[24,25] In selected clinically asymptomatic patients with *IDH*-mutant and occasionally 1p/19q codeleted grade II gliomas, treatment was withheld and a wait-and-scan attitude preferred.[26]

Treatment response was evaluated according to contemporary guidelines at the time of patient enrollment.[12,27] For the sake of objective comparability, all MRI scans have been reevaluated according to current Response Assessment in Neuro-Oncology criteria.[12] Before initiation of salvage treatment, a re-biopsy was done for verification of tumor progression. In case of an assumed pseudoprogression after chemotherapy/radiotherapy, another ^{18}F-FET-PET examination was performed.[28,29] Recommendations for salvage treatment were given by the interdisciplinary tumor board.

Statistical Analysis

The reference point for this study was the date of initial stereotactic biopsy. Date of last follow-up was July 2017. The sample size of our initial intermediate-term analysis was based on the presumption of an unadjusted hazard ratio of at least 2 for any form of decreasing TAC to be associated with tumor progression. In the current long-term analysis, we presumed an unadjusted hazard ratio of at least 2 for any form of decreasing TAC to be associated with death. Given an accrual period of 48 months and a total time of 139 months, a sample size of at least 36 tumors in each of the 2 TAC groups (increasing vs decreasing) would be also sufficient to support/reject the study hypothesis with a statistic power of 80%. Progression-free survival, overall survival (OS), and post-recurrence survival (PRS) were analyzed with the Kaplan–Meier method and compared with the log-rank statistic. Prognostic factors were obtained from univariate and multivariate proportional hazards models. First, the importance of each variable was tested univariately. Second, all variables were fitted together. The final models contained only variables associated with PFS, OS, or PRS after adjustment for the effects of the other variables. In case of intercorrelated

covariates, alternative models with inclusion of either of these covariates were tested and compared by computing the maximized likelihoods. Adjusted survival curves were computed to demonstrate the prognostic impact of the selected covariates. Logistic regression models were used to elucidate the association of TACs with biospecimen-derived and clinically derived biomarkers. The distribution of continuously scaled variables was analyzed with the Wilcoxon test. For dichotomized variables, the chi-squared statistics or Fisher's exact test (in case of small sample sizes) was used. All calculations were performed using SAS software v9.2.

Results

Overall, 52 *IDH*-mutant WHO grade II gliomas (including 19 tumors with 1p/19q codeletion), 17 *IDH*-mutant grade III gliomas (9 with 1p/19q codeletion), and 29 *IDH*-wildtype tumors (7 grade II, 18 grade III gliomas, and 4 glioblastomas) were diagnosed (overall grades III/IV gliomas: 40%). Among the *IDH*-wildtype tumors, an additional *TERT* promoter mutation was seen in 5 grade II and 12 grade III gliomas (Table 1). A homogeneous increasing, homogeneous decreasing, and mixed TAC pattern was seen in 51, 28, and 19 patients, respectively. Median TTP_{min} was 35 min (range 35–35 min) for homogeneous increasing, 17.5 min (range 7.5–25 min) for mixed TAC, and 12.5 min (range 4–25 min) for homogeneous decreasing TAC tumors ($P < 0.0001$). No tumor with decreasing TAC (either focally or homogeneously) exhibited a TTP_{min} value >25 min. The median TTP_{min} for these decreasing TAC tumors was 12.5 min, which was used as the cutoff value for further stratification of decreasing TAC tumors. In prognostic models, a 3-scaled TTP_{min}-based classifier was used: TTP_{min} > 25 min (the long TTP_{min} subgroup) versus $TTP_{min} \leq 25$ and > 12.5 min (the intermediate TTP_{min} subgroup) versus $TTP_{min} \leq 12.5$ min (the short TTP_{min} subgroup).

Median follow-up of the survivors was 90 months (range, 32–132 mo). Seventy-nine (80.6%) patients experienced tumor progression and 50 (51.0%) patients died. Twenty out of 52 *IDH*-mutant grade II patients suffered from tumor progression with biopsy-proven malignant transformation (toward WHO grades III/IV histology). In 13 of these patients, a follow-up ^{18}F-FET-PET was available at the time of malignant transformation, indicating a corresponding shift in qualitative (quantitative) TAC measurements from an initially homogeneous increasing TAC (long TTP_{min}) toward a mixed TAC pattern (intermediate TTP_{min}) in 9 and toward a homogeneous decreasing TAC pattern (short TTP_{min}) in 4 tumors. Overall, median PFS, OS, and PRS of the study population were 40 months (95% CI: 28–52 mo), 84 months (95% CI: 51–117), and 20 months (95% CI: 8–32), respectively.

Prognostic Models

A compilation of the results of univariate and multivariate analyses for PFS, OS, and PRS is shown in Table 2. Multivariately, outcome could be similarly precisely predicted by a biospecimen-derived and the 2 imaging-derived models including either qualitative TAC assessment or quantitative TTP_{min} measurements: In the multivariate biospecimen-derived model WHO grade (II vs III/IV, $P < 0.0001$) and *IDH*-mutational status ($P < 0.001$) were independently associated with PFS and OS. In the 2 alternative imaging-derived multivariate models, the 1p/19q codeletion status ($P < 0.01$) and either TAC patterns ($P < 0.0001$) or the 3-scaled TTP_{min} classifier ($P < 0.0001$) turned out to be significant predictors for PFS and OS. The unadjusted hazard ratio of any form of decreasing TAC for tumor progression and death was 3.4 (95% CI: 2.17–5.6) and 5.5 (95% CI: 2.8–10.6), respectively. For the 3-scaled TAC classifier, we found a stepwise risk increase of 1.8 (95% CI: 1.36–2.3) for tumor progression and 1.9 (95% CI: 1.39–2.6) for death. Similar risk estimations could be obtained from TTP_{min} measurements (see Table 2). In univariable analyses, the impact of TTP_{min} on PFS was even more powerful than qualitative TAC assessment. The adjusted (unadjusted) 5-year survival for *IDH*-mutant grade II, *IDH*-mutant grade III, and *IDH*-wildtype tumors was 86.8% (88.4%), 47.6% (50.0%), and 8.0% (14.0%), and it was 85.0% (82.0%), 47.0% (50.0%), and 19.0% (25.0%) for homogeneous increasing, mixed, and decreasing TAC tumors, respectively. Tumors exhibiting long, intermediate, and short TTP_{min} measurements experienced adjusted (unadjusted) 5-year survival of 79.0% (82.0%), 53.0% (53.0%), and 19.0% (22.0%), respectively. Differences between each of the 3 clusters of the biospecimen- and imaging-derived models were significant (Table 1 and Figs.1 and 2) ($P < 0.001$). Corresponding clusters of each model exhibited comparable outcome. Outcome of *IDH*-wildtype tumors, however, tended to be slightly worse than in both the homogeneous decreasing TAC and the short TTP_{min} tumors. This difference did not reach significance ($P = 0.8$).

Correlations Between Biospecimen- and Nuclear Imaging–Derived Variables

Forty-seven (90.4%) of the 52 *IDH*-mutant grade II gliomas gathered in the homogeneous increasing TAC, all 17 *IDH*-mutant grade III gliomas in the mixed TAC, and all 22 *IDH*-wildtype grades III/IV gliomas in the homogeneous decreasing TAC group ($P < 0.001$). Likewise, 47 (90.4%) *IDH*-mutant grade II gliomas gathered in late, 12 (71%) of the *IDH*-mutant grade III gliomas in the intermediate, and 20 (91%) of the *IDH*-wildtype grades III/IV gliomas in the short TTP_{min} group ($P < 0.001$). Overall, TTP_{min} was longer for the *IDH*-mutant tumors. This was true for the overall population (median TTP_{min} in *IDH*-mutant vs -wildtype tumors: 35 min vs 12.5 min; $P < 0.0001$) as well as for the grades III/IV subpopulation (median 17.5 min vs 12.5 min; $P < 0.001$).

Sensitivity, specificity, and positive predictive value of the homogeneous increasing and the mixed TAC patterns to detect an *IDH*-mutant glioma (grade II or III) was 94.2%, 83.0%, and 93.0%, respectively. The corresponding values for the late and intermediate TTP_{min} classes were 91.3%, 76%, and 90%. The difference was statistically not significant ($P = 0.9$). Overall, both kinetic classification schemes were highly intercorrelated ($P < 0.0001$). *IDH*-wildtype, *TERT* positive, grade II gliomas ($n = 5$) were found in each of the TAC groups and exhibited also variable TTP_{min}

Table 1 Detailed characterization of the 3 TAC groups, including distribution according to the new 2016 WHO classification scheme, TTP_{min} analysis, treatment at initial diagnosis/progression, and corresponding outcome parameters

	(a) Homogeneous Increasing TAC ($n = 51$)	(b) Mixed TAC ($n = 19$)	(c) Homogeneous Decreasing TAC ($n = 28$)	*P*-value
Integrated WHO classification 2016				
Grade II				
IDH-mutant astrocytoma	33	-	-	
IDH-mutant 1p/19q codel.	14	1	4	a vs. b: <0.001
IDH-wildtype TERT neg.	2	-	-	a vs. c: <0.001
IDH-wildtype TERT pos.	2	1	2	b vs. c: >0.05
Grade III				
IDH-mutant astrocytoma	-	8	-	
IDH-mutant 1p/19q codel.	-	9	-	a vs. b: <0.001
IDH-wildtype TERT neg.	-	-	6	a vs. c: <0.001
IDH-wildtype TERT pos.	-	-	12	b vs. c: >0.05
Grade IV				
IDH-wildtype TERT pos.	-	-	4	a vs. c: <0.05
				b vs. c: >0.05
Time-to-peak				
TTP_{min} [min.]	35	17.5	12.5	a vs. b: <0.001
Median [range]	[35–35]	[7.5–25]	[4–25]	a vs. c: <0.001
				b vs. c: <0.001
Treatment at first diagnosis				
None	17 (33%)	1 (5%)	1 (4%)	a vs. b/c: <0.05
Local only (Surg/SBT)	11 (22%)	1 (5%)	1 (4%)	a vs. b/c: <0.05
CTx/RTx (± Surg/SBT)	23 (45%)	17 (90%)	26 (93%)	a vs. b/c: <0.001
Events				
Progression, *n*	34 (67%)	18 (95%)	27 (96%)	a vs. b/c: <0.05
Death, *n*	15 (29%)	11 (58%)	24 (86%)	a vs. b/c: <0.05
Treatment at progression				
Local only (Surg or SBT)	4 (12%)	0 (0%)	0 (0%)	a vs. b/c: >0.05
CTx/RTx (±Surg/SBT)	30 (88%)	16 (89%)	22 (81%)	a vs. b/c: >0.05
Palliative care	0 (0%)	2 (11%)	5 (19%)	a vs. b: >0.05
				a vs. c: <0.05
Progression-free survival				
2 y	86%	50%	29%	a vs. b: <0.001
5 y	48%	22%	14%	a vs. c: <0.001
				b vs. c: <0.05
Overall survival				
2 y	94%	83%	43%	a vs. b: <0.001
5 y	82%	50%	25%	a vs. c: <0.001
				b vs. c: <0.05
Post-recurrence survival				
2 y	73%	47%	19%	a vs. b: =0.05
5 y	51%	25%	7%	a vs. c: <0.001
				b vs. c: <0.05

Codel., codeletion; pos., positive; neg., negative; CTx, chemotherapy; RTx, radiotherapy; SBT, stereotactic brachytherapy; Surg, microsurgical resection.

Table 2 Prognostic factors for PFS, OS, and PRS in the univariate and for PFS and OS in the multivariate analyses

Univariate Analysis						
Factor	PFS		OS		PRS	
	P	Hazard Ratio (95% CI)	*P*	Hazard Ratio (95% CI)	*P*	Hazard Ratio (95% CI)
Age						
≤50 y vs >50 y	0.005	0.5 (0.3–0.8)	<0.001	0.3 (0.2–0.5)	<0.0001	0.3 (0.2- 0.6)
KPS						
≤80 vs >80	<0.001	3.1 (1.7–5.9)	<0.001	3.8 (1.9–7.8)	0.003	3.0 (1.5- 6.1)
Sex						
Male vs female	0.33	0.8 (0.5–1.3)	0.1	0.6 (0.3–1.1)	0.4	0.7 (0.6–1.3)
Tumor volume						
≤35 mL vs >35 mL	0.4	0.8 (0.5–1.3)	0.8	0.9 (0.5–1.7)	0.9	1.0 (0.9–1.1)
SUVmax						
≤2.3 vs >2.3	0.43	0.8 (0.5–1.3)	0.6	0.9 (0.5–1.6)	0.4	0.8 (0.4–1.4)
Resection						
Yes vs no	0.3	1.3 (0.8–2.1)	0.7	1.1 (0.6–2.1)	0.4	1.2 (0.7–2.1)
TAC pattern						
Homogeneous decreasing vs mixed vs homogeneous increasing	*0.001*	*1.7 (1.3–2.2)*	*<0.001*	*1.7 (1.3–2.4)*	*0.003*	*1.7 (1.2–2.4)*
TTP_{min}						
>25 min. vs 12.5 < t ≤ 25 min. vs ≤12.5 min.	<0.0001	2.3 (1.7–2.9)	<0.0001	2.7 (1.9–3.7)	0.08	1.9 (0.9–3.3)
Histology						
Astrocytic vs oligodendroglial tumors	0.01	2.1 (1.2–3.7)	0.01	2.9 (1.3–6.6)	0.03	2.2 (1.3–4.1)
WHO grade						
II vs III/IV	<0.001	0.2 (0.1–0.4)	<0.001	0.2 (0.1–0.3)	0.0001	0.3 (0.13–0.5)
Ki-67						
≤7% vs >7%	<0.001	0.3 (0.2–0.5)	<0.001	0.2 (0.1–0.3)	0.001	0.4 (0.2–0.7)
***IDH* mutational status**						
Wildtype vs *mutant*	<0.001	3.6 (2.2–5.8)	<0.001	7.4 (4–13.6)	<0.0001	5.9 (3.1–11.4)
***1p/19q* codeletion**						
No vs yes	0.01	2.1 (1.2–3.6)	0.014	2.8 (1.2–6.3)	0.2	1.6 (0.7–3.3)
***MGMT* promoter status**						
Unmethylated vs methylated	0.09	1.7 (0.9–3)	0.01	2.5 (1.3–4.9)	0.02	2.3 (1.1–4.5)
***TERT* mutational status**						
Positive vs negative	0.7	0.8 (0.4–1.9)	0.67	0.8 (0.4–1.9)	0.4	0.9 (0.3–1.7)
Multivariate analysis						
Factor	PFS		OS			
	P	Hazard Ratio (95% CI)	*P*	Hazard Ratio (95% CI)		
Imaging-derived Model 1						
TAC pattern						
Homogeneous decreasing vs mixed vs homogeneous increasing	<0.0001	2.1 (1.6–2.8)	<0.0001	2.6 (1.8–3.9)		
***1p/19q* codeletion**						
No vs yes	0.0001	3.0 (1.7–5.2)	<0.0001	5.0 (2.2–11.1)		
Imaging-derived Model 2						
TTP_{min}						
>25 min. vs 12.5 < t ≤ 25 min. vs ≤12.5 min.	<0.0001	2.2 (1.7–2.8)	<0.0001	2.6 (1.9–3.6)		

Table 2 *Continued*

Multivariate analysis				
Factor	PFS		OS	
	P	Hazard Ratio (95% CI)	*P*	Hazard Ratio (95% CI)
***1p/19q* codeletion**				
No vs yes	0.002	2.3 (1.4–3.8)	0.002	3.3 (1.6–8.1)
Biospecimen-derived Model				
WHO grade				
II vs III/IV	<0.0001	0.3 (0.2–0.5)	<0.0001	0.3 (0.1–0.5)
***IDH*-mutational status**				
Wildtype vs *mutant*	0.0005	2.5 (1.5–4.1)	<0.0001	4.8 (2.6–9)

values (see Supplementary Table 1). These tumors were associated with both significantly increased age (median 63 y vs 36 y; $P = 0.03$) and worse outcome—median PFS: 15 months (range: 4–26 mo) vs 68 months (range: 54–82); $P = 0.001$; median OS: 45 months (range: 28–62 mo) vs not reached; $P < 0.001$. In contrast, *IDH*-wildtype, *TERT* negative grade II gliomas ($n = 2$) did not differ in terms of age and outcome from their *IDH*-mutant counterparts and exclusively referred to both the increasing TAC and the late TTP_{min} groups. No correlation was found between TTP_{min} measurements and the 1p/19q status (codeleted vs non-codeleted tumors: median 30 min vs 35 min, $P > 0.05$). Grade II 1p/19q codeleted tumors were sometimes characterized by unfavorable TAC measurements (ie, 4 grade II 1p/19q codeleted tumors were categorized as homogeneous decreasing TAC tumors and another one as mixed TAC tumor). TTP_{min} measurements of these 5 tumors indicated intermediate TTP_{min} in 4 and short TTP_{min} in 1 patient. None of these patients experienced unfavorable clinical outcome. Three out of 9 grade III codeleted tumors were categorized as short TTP_{min} tumors, whereas all 9 tumors were exclusively found in the mixed TAC group. Discordant findings concerned 2 further *IDH*-mutant grade III mixed TAC tumors categorized as short TTP_{min} gliomas and another 2 *IDH*-wildtype grade III homogeneous decreasing TAC tumors categorized as intermediate TTP_{min} gliomas.

In multivariate logistic regression analysis, a WHO grades III/IV tumor was associated with decreasing TAC ($P < 0.0001$). An alternative model with inclusion of TTP_{min} measurements indicated *IDH*-wildtype status ($P < 0.001$) and WHO grades III/IV ($P < 0.01$) independently to be associated with a $TTP_{min} \leq 12.5$ min.

Treatment

Initial and salvage treatment concepts are summarized in Table 1 and the Supplementary Table. Early radiotherapy and/or chemotherapy were more frequently applied in the mixed and the homogeneous decreasing TAC groups ($P < 0.001$), whereas localized treatment strategies only (such as resection or brachytherapy) were preferred for circumscribed homogeneous increasing TAC tumors ($P = 0.03$). Within each TAC group the applied treatment (localized vs irradiation and/or chemotherapy) regimen did not gain prognostic impact.

Nineteen patients with *IDH*-mutant grade II gliomas underwent careful observation (89.5% of these patients exhibited an increasing TAC pattern/long TTP_{min}). Associated PFS tended to be shorter than for the corresponding early treatment group (median PFS, 37 mo [95% CI: 22–52 mo] vs 70 months [95% CI: 59–81 mo]; $P = 0.07$). However, delayed radio- and/or chemotherapy at the time of tumor progression was associated with longer PRS in the wait-and-scan group (median PRS: 41 mo [95% CI: not reached] vs 29 months [95% CI: 11–46 mo]; $P = 0.05$), resulting in comparable OS in both the early and delayed treatment groups (Table 1).

Discussion

^{18}F-FET-PET data processing including TAC analysis has been shown to be a rather robust and reproducible method for glioma grading.[20] Using ^{18}F-FET-PET–guided serial stereotactic molecular biopsy technique we recently described 3 intratumoral TAC patterns in Gd-negative gliomas, each correlating with distinct histopathological and molecular-genetic profiles.[16,17] This is to our knowledge the first prospective sufficiently powered long-term study analyzing the risk of death in Gd-negative gliomas stratified for TAC patterns, WHO grade, and molecular biomarker profiles. We found an approximately 5-fold increased unadjusted risk of death in case of any form of decreasing TAC compared with homogeneous increasing TAC tumors. Our data indicate additionally that in qualitative TAC analysis, not only the separation between increasing and decreasing TAC but also the consideration of their spatial distribution (ie, mixed TAC patterns) within the tumor landscape matter for prognostic evaluation resulting in the 3-scaled TAC pattern-based prognostic classifier of this study.

As some studies have pointed to the prognostic impact of TTP_{min} measurements in glioma, we additionally performed post-hoc analyses of TTP_{min} of each tumor.[18] We found 3-scaled qualitative TAC and quantitative TTP_{min} measurements to be highly intercorrelated. Homogeneous

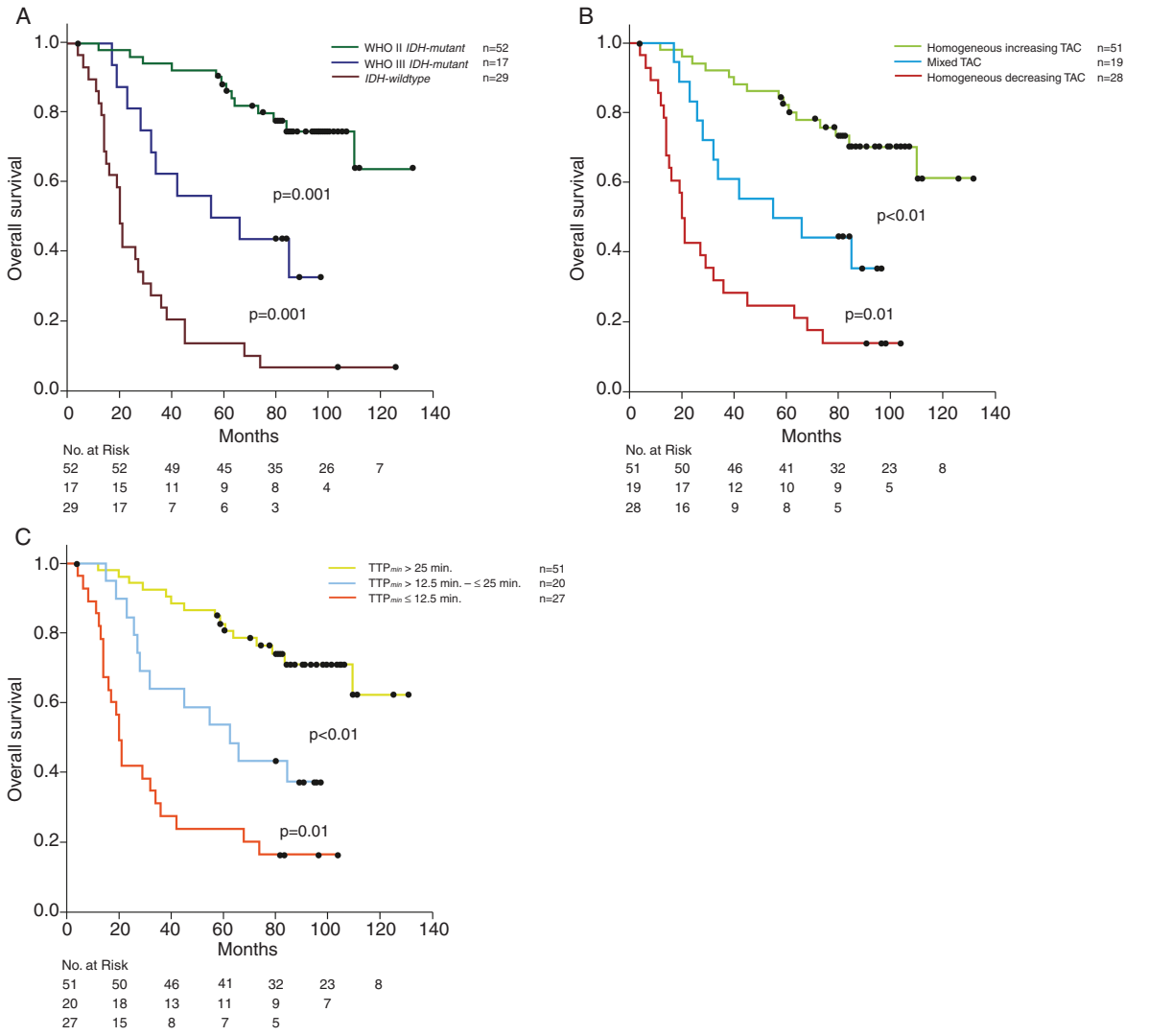

Fig. 1 Kaplan–Meier curves of overall survival for the entire study population stratified by WHO grade and molecular-genetic markers according to the new 2016 WHO classification scheme (A), TAC patterns (B) and TTP_{min} analysis (C). Significant differences in OS were shown in each of the 3-scaled curves.

decreasing TAC (homogeneous increasing TAC) tumors experienced the shortest (longest) median TTP_{min} measurements. Median TTP_{min} of mixed TAC tumors was in between. Similar to the 3-scaled qualitative classifier, the distribution of the TTP_{min} values also allowed a 3-scaled stratification (>25 min vs >12.5 min and ≤25 min vs ≤12.5 min) of the study population. We here tested and compared the usefulness of this new quantitative retrospectively obtained TTP_{min} classifier with the qualitative TAC data.

We demonstrate that models relying either on nuclear imaging-derived (qualitatively obtained 3-scaled TAC pattern/3-scaled TTP_{min} classification) or biospecimen-derived biomarkers predicted nearly identical survival rates. Homogeneous increasing TAC tumors and those gliomas exhibiting a TTP_{min} > 25 min did as well as *IDH*-mutant grade II gliomas and those gliomas with homogeneous decreasing TAC/TTP_{min} ≤ 12.5 min as poor as *IDH*-wildtype tumors. *IDH*-mutant grade III, mixed TAC tumors and those exhibiting a TTP_{min} between 12.5 and 25.0 min had an intermediate prognosis. Whereas a 1p/19q codeletion was not considered in the biospecimen-derived prognostic model (probably because of the relatively small sample size of codeleted tumors), it gained influence in both kinetic models. It cannot be excluded, however, that the impact of the 1p/19q status was overestimated in the imaging-derived models and was triggered mainly by some grade II oligodendrogliomas with favorable outcome scores resembling found within the decreasing (short/intermediate) TAC (TTP_{min}) group. Limitations of TAC analyses in grade II oligodendrogliomas have already been reported in the literature and have become apparent also in this study for TTP_{min} measurements.[30] Only a few tumors did not fit the

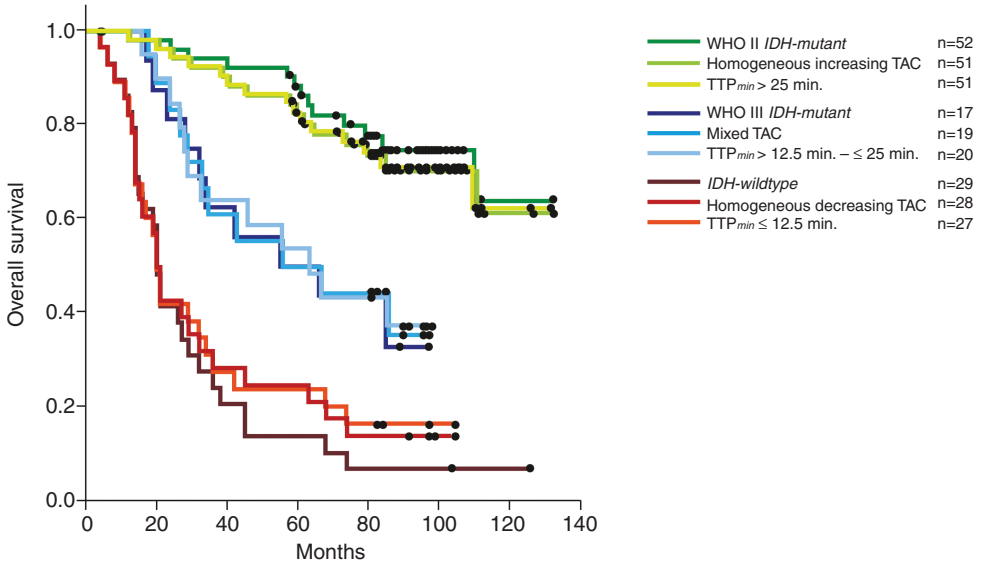

Fig. 2 Kaplan–Meier curves of OS stratified by WHO grade and molecular-genetic markers did not significantly differ from those stratified by TAC patterns and TTP_{min} analysis, as seen in the overlapping view. The differences in each of the 3 clusters were significant.

described correlation schemes. Beyond the 1p/19q codeleted tumors, *IDH*-wildtype tumors with/without an additional *TERT* mutation were not unequivocally characterized as malignant gliomas. Apparently these lesions experienced heterogeneous tumor characteristics, which cannot be unequivocally classified by both qualitative and quantitative TAC analyses. More data are necessary to elucidate whether TAC analyses might provide additional information relevant for prognosis of these rather rare grade II glioma subpopulations.[6] Notably, the detected powerful impact of the 3-scaled TTP_{min} classes derived from retrospective analyses and must therefore be interpreted cautiously. Further prospective evaluation is needed.

We demonstrated further that *IDH*-mutant tumors experienced longer TTP_{min} times, which was independent of tumor grade. Other studies have already reported a similar correlation but did not adjust their findings for the effects of tumor grade.[18,31] Whereas a higher tumor grade turned out to be the main determinant for the evolvement of a decreasing TAC pattern, TTP_{min} measurements seem to be more sensitive to identify differences among decreasing TACs of distinct tumors not recognizable by qualitative TAC analyses. Longer TTP_{min} times in *IDH*-mutant grade III tumors might point to less aggressiveness of these tumors compared with their *IDH*-wildtype counterparts. It will be a matter of further research to elucidate correlations between the *IDH* mutational status, the expression of the L-system amino acid transporter (LAT) in tumor vessels, as well as microvessel density (which can be seen in malignant gliomas as well as sometimes in grade II oligodendrogliomas). All these factors are increasingly considered important for both rapid influx and early wash-out effects of ^{18}F-FET in glioma.[32–36]

Mixed TAC tumors, which experienced an intermediate prognosis in this series, represent the diagnostically most challenging subgroup among the Gd-negative tumors. These tumors might be easily misclassified as WHO grade II gliomas in case of non-representative resection/biopsy strategies resulting in undertreatment and potential worsening of the overall prognosis. Thus, initial characterization of the Gd-negative gliomas by molecular imaging such as ^{18}F-FET-PET is indispensable to identify these heterogeneously composed tumors and to guide biopsy/resection for representative tissue sampling either initially at the time of the first presentation or when tumor progression is assumed. According to our data, homogeneous increasing TAC tumors could evolve to mixed TAC or even homogeneous decreasing TAC tumors during the tumor progression process, which was always associated with biopsy-proven malignant transformation.[29,37] These changes also became evident in quantitative TAC analyses, indicating a shift from long TTP_{min} to the intermediate or short TTP_{min} values.

Given the strong correlation between the biospecimen-derived and imaging-derived models, it was not surprising that TAC patterns and treatment were highly intercorrelated. Patients with mixed (intermediate TTP_{min}) or homogeneous decreasing TAC (short TTP_{min}) patterns received the most dense treatment protocols, whereas patients undergoing localized treatment or even a wait-and-scan attitude typically belonged to the homogeneous increasing TAC/long TTP_{min} group. The depiction of increasing TAC tumors either as circumscribed or diffuse might support treatment decisions in favor of a more or less localized therapy, thereby in the future possibly improving the risk/benefit profile of the applied treatment. This hypothesis needs further prospective evaluation.

A considerable number of patients mainly with homogeneous increasing TAC (long TTP_{min}) tumors received delayed treatment. This patient subpopulation had smaller tumor volumes and no/minimal clinical deficits and was younger compared with those undergoing early treatment. PFS was shorter after wait-and-scan. This disadvantage, however, was compensated by longer PRS after delayed treatment, resulting in similarly long survival in the early and delayed treatment groups. This new finding should be prospectively evaluated. Our data suggest that in highly selected asymptomatic patients <40 years of age (most likely excluding *IDH*-wildtype, *TERT* positive tumors) with supratentorial, unresectable, homogeneous increasing TAC/long TTP_{min} tumors, biopsy should be performed but treatment may be withheld until tumor progression occurs.

Conclusion

The prognosis of Gd-negative gliomas can be described by qualitative and probably similarly precisely also by quantitative TAC assessment without knowledge of tumor grade and *IDH* mutational status. Limitations of the respective TAC models concerned low-grade oligodendrogliomas (sometimes classified as malignant gliomas) and *IDH*-wildtype, *TERT* positive grade II astrocytomas (sometimes described by a favorable kinetic pattern). TAC analyses provide the possibility to guide biopsy and resection particularly in heterogeneously composed tumors. It enables further adjustment of invasiveness, time point of diagnostic procedures, and treatment to the metabolic profile of the tumor under consideration.

Supplementary material

Supplementary material is available online at *Neuro-Oncology* (http://neuro-oncology.oxfordjournals.org/).

Funding

Parts of this study were funded by German Cancer Aid (Deutsche Krebshilfe), grant number 70-3163-Wi 3.

Acknowledgments

No prior or subsequent publication. Preliminary analyses of this prospective study have been published before. This paper provides the long-term follow-up data within the framework of the 2016 WHO classification of gliomas. It is not under consideration, in press, or being published elsewhere.

Conflict of interest statement. No potential conflicts of interest have to be disclosed.

References

1. Weller M, van den Bent M, Tonn JC, et al; European Association for Neuro-Oncology (EANO) Task Force on Gliomas. European Association for Neuro-Oncology (EANO) guideline on the diagnosis and treatment of adult astrocytic and oligodendroglial gliomas. *Lancet Oncol*. 2017;18(6):e315–e329.
2. van den Bent MJ, Snijders TJ, Bromberg JE. Current treatment of low grade gliomas. *Memo*. 2012;5(3):223–227.
3. Pouratian N, Schiff D. Management of low-grade glioma. *Curr Neurol Neurosci Rep*. 2010;10(3):224–231.
4. Forst DA, Nahed BV, Loeffler JS, Batchelor TT. Low-grade gliomas. *Oncologist*. 2014;19(4):403–413.
5. Louis DN, Perry A, Reifenberger G, et al. The 2016 World Health Organization classification of tumors of the central nervous system: a summary. *Acta Neuropathol*. 2016;131(6):803–820.
6. Eckel-Passow JE, Lachance DH, Molinaro AM, et al. Glioma groups based on 1p/19q, IDH, and TERT promoter mutations in tumors. *N Engl J Med*. 2015;372(26):2499–2508.
7. Buckner J, Giannini C, Eckel-Passow J, et al. Management of diffuse low-grade gliomas in adults—use of molecular diagnostics. *Nat Rev Neurol*. 2017;13(6):340–351.
8. Yan H, Parsons DW, Jin G, et al. IDH1 and IDH2 mutations in gliomas. *N Engl J Med*. 2009;360(8):765–773.
9. Claus EB, Walsh KM, Wiencke JK, et al. Survival and low-grade glioma: the emergence of genetic information. *Neurosurg Focus*. 2015;38(1):E6.
10. Scott JN, Brasher PM, Sevick RJ, Rewcastle NB, Forsyth PA. How often are nonenhancing supratentorial gliomas malignant? A population study. *Neurology*. 2002;59(6):947–949.
11. Pallud J, Capelle L, Taillandier L, et al. Prognostic significance of imaging contrast enhancement for WHO grade II gliomas. *Neuro Oncol*. 2009;11(2):176–182.
12. van den Bent MJ, Wefel JS, Schiff D, et al. Response assessment in neuro-oncology (a report of the RANO group): assessment of outcome in trials of diffuse low-grade gliomas. *Lancet Oncol*. 2011;12(6):583–593.
13. Cui Y, Tha KK, Terasaka S, et al. Prognostic imaging biomarkers in glioblastoma: development and independent validation on the basis of multiregion and quantitative analysis of MR images. *Radiology*. 2016;278(2):546–553.
14. Fan GG, Deng QL, Wu ZH, Guo QY. Usefulness of diffusion/perfusion-weighted MRI in patients with non-enhancing supratentorial brain gliomas: a valuable tool to predict tumour grading? *Br J Radiol*. 2006;79(944):652–658.
15. Albert NL, Weller M, Suchorska B, et al. Response assessment in Neuro-Oncology working group and European Association for Neuro-Oncology recommendations for the clinical use of PET imaging in gliomas. *Neuro Oncol*. 2016;18(9):1199–1208.
16. Kunz M, Thon N, Eigenbrod S, et al. Hot spots in dynamic (18)FET-PET delineate malignant tumor parts within suspected WHO grade II gliomas. *Neuro Oncol*. 2011;13(3):307–316.
17. Thon N, Kunz M, Lemke L, et al. Dynamic ^{18}F-FET PET in suspected WHO grade II gliomas defines distinct biological subgroups with different clinical courses. *Int J Cancer*. 2015;136(9):2132–2145.
18. Suchorska B, Giese A, Biczok A, et al. Identification of time-to-peak on dynamic ^{18}F-FET-PET as a prognostic marker specifically in IDH1/2 mutant diffuse astrocytoma. *Neuro Oncol*. 2018;20(2):279–288.
19. Albert NL, Winkelmann I, Suchorska B, et al. Early static (18) F-FET-PET scans have a higher accuracy for glioma grading than the standard 20-40 min scans. *Eur J Nucl Med Mol Imaging*. 2016;43(6):1105–1114.

20. Filss CP, Albert NL, Böning G, et al. O-(2-[18F]fluoroethyl)-L-tyrosine PET in gliomas: influence of data processing in different centres. *EJNMMI Res*. 2017;7(1):64.
21. Eigenbrod S, Trabold R, Brucker D, et al. Molecular stereotactic biopsy technique improves diagnostic accuracy and enables personalized treatment strategies in glioma patients. *Acta Neurochir (Wien)*. 2014;156(8):1427–1440.
22. Kreth FW, Faist M, Grau S, Ostertag CB. Interstitial 125I radiosurgery of supratentorial de novo WHO grade 2 astrocytoma and oligoastrocytoma in adults: long-term results and prognostic factors. *Cancer*. 2006;106(6):1372–1381.
23. Wick W, Hartmann C, Engel C, et al. NOA-04 randomized phase III trial of sequential radiochemotherapy of anaplastic glioma with procarbazine, lomustine, and vincristine or temozolomide. *J Clin Oncol*. 2009;27(35):5874–5880.
24. Stupp R, Mason WP, van den Bent MJ, et al; European Organisation for Research and Treatment of Cancer Brain Tumor and Radiotherapy Groups; National Cancer Institute of Canada Clinical Trials Group. Radiotherapy plus concomitant and adjuvant temozolomide for glioblastoma. *N Engl J Med*. 2005;352(10):987–996.
25. Hartmann C, Hentschel B, Wick W, et al. Patients with IDH1 wild type anaplastic astrocytomas exhibit worse prognosis than IDH1-mutated glioblastomas, and IDH1 mutation status accounts for the unfavorable prognostic effect of higher age: implications for classification of gliomas. *Acta Neuropathol*. 2010;120(6):707–718.
26. Whittle IR. What is the place of conservative management for adult supratentorial low-grade glioma? *Adv Tech Stand Neurosurg*. 2010;35:65–79.
27. Macdonald DR, Cascino TL, Schold SC Jr, Cairncross JG. Response criteria for phase II studies of supratentorial malignant glioma. *J Clin Oncol*. 1990;8(7):1277–1280.
28. Galldiks N, Law I, Pope WB, Arbizu J, Langen KJ. The use of amino acid PET and conventional MRI for monitoring of brain tumor therapy. *Neuroimage Clin*. 2017;13:386–394.
29. Galldiks N, Stoffels G, Filss C, et al. The use of dynamic O-(2-18F-fluoroethyl)-l-tyrosine PET in the diagnosis of patients with progressive and recurrent glioma. *Neuro Oncol*. 2015;17(9):1293–1300.
30. Jansen NL, Schwartz C, Graute V, et al. Prediction of oligodendroglial histology and LOH 1p/19q using dynamic [(18)F]FET-PET imaging in intracranial WHO grade II and III gliomas. *Neuro Oncol*. 2012;14(12):1473–1480.
31. Jansen NL, Suchorska B, Wenter V, et al. Dynamic 18F-FET PET in newly diagnosed astrocytic low-grade glioma identifies high-risk patients. *J Nucl Med*. 2014;55(2):198–203.
32. Zhao Y, Wang L, Pan J. The role of L-type amino acid transporter 1 in human tumors. *Intractable Rare Dis Res*. 2015;4(4):165–169.
33. Haining Z, Kawai N, Miyake K, et al. Relation of LAT1/4F2hc expression with pathological grade, proliferation and angiogenesis in human gliomas. *BMC Clin Pathol*. 2012;12:4.
34. Stockhammer F, Plotkin M, Amthauer H, van Landeghem FK, Woiciechowsky C. Correlation of F-18-fluoro-ethyl-tyrosin uptake with vascular and cell density in non-contrast-enhancing gliomas. *J Neurooncol*. 2008;88(2):205–210.
35. Wyss MT, Hofer S, Hefti M, et al. Spatial heterogeneity of low-grade gliomas at the capillary level: a PET study on tumor blood flow and amino acid uptake. *J Nucl Med*. 2007;48(7):1047–1052.
36. Verger A, Stoffels G, Bauer EK, et al. Static and dynamic ^{18}F-FET PET for the characterization of gliomas defined by IDH and 1p/19q status. *Eur J Nucl Med Mol Imaging*. 2018;45(3):443–451.
37. Galldiks N, Stoffels G, Ruge MI, et al. Role of O-(2-18F-fluoroethyl)-L-tyrosine PET as a diagnostic tool for detection of malignant progression in patients with low-grade glioma. *J Nucl Med*. 2013;54(12):2046–2054.